Origin of the Transition State on the Free Energy Surface: Intramolecular Proton Transfer Reaction of Glycine in Aqueous Solution

Masataka Nagaoka* and Naoto Okuyama-Yoshida†

Institute for Fundamental Chemistry, 34-4, Takano-Nishihiraki-cho, Sakyo-ku, Kyoto 606, Japan

Tokio Yamabe

Division of Molecular Engineering, Kyoto University, Sakyo-ku, Kyoto 606, Japan

Received: June 8, 1998

Not only to elucidate the origin of the reaction barrier in liquid phase, i.e., the free energy of activation, but also to locate the proper transition state (TS) for a chemical reaction, the molecular dynamics method and the free energy perturbation theory have been applied to the intramolecular proton transfer reaction of glycine in aqueous solution, i.e., the zwitterion (ZW), to the neutral form (NF). The potential energy surface varies drastically as its environment changes from gas phase to aqueous solution, and experimentally, the existence of an *entropy* barrier is also suggested due to the solvent molecules. In this study, it is reported that the TS on the free energy surface (FES) corresponds approximately to the geometry at $s \approx 0.66$ amu$^{1/2}$ bohr, where s denotes the intrinsic reaction coordinate (IRC) for the gas-phase reaction, and therefore, the TS geometry is completely different from that for the gas phase. The free energy difference between ZW and NF is 8.46 $\pm$ 1.45 kcal/mol, and then the free energy of activation of ZW is 16.85 $\pm$ 1.36 kcal/mol at the temperature 300 K, both of which are in very good agreement with the experimental values. Further, the entropy contribution to the free energy change increases almost monotonously along the IRC, while the enthalpy contribution has a maximum at $s \approx 0.6$ amu$^{1/2}$ bohr, being understood as the origin of the free energy of activation. By the interaction energy distribution and the radial distribution functions, it is shown that solvent water molecules interact with ZW more strongly than both TS and NF, especially at both the positive amino and negative carboxyl groups. Therefore, from a microscopic point of view, the reaction barrier in aqueous solution is clearly explained by the fact that as the forward reaction (ZW $\rightarrow$ NF) proceeds, the Coulomb interaction between the charged groups of ZW and solvent water molecules becomes weaker while the intramolecular potential energy is stabilized compensatorily to form a free energy maximum.

I. Introduction

To predict rates for complex chemical reactions in solution is one primary goal of theoretical chemistry. Within the framework of transition-state theory (TST),[1−4] knowledge of the free energy surface (FES) around a transition state (TS) and a reactant state (RS), i.e., the free energy of activation, is sufficient to determine the rate constant k_{TST} for the reaction and thereby the magnitude of the overall time required for the reactant to climb the barrier from an equilibrium state. The FES consists of two terms: one for the reacting system and the other for the variation through the free energy of solvation.[5,6] The former reflects the intrinsic part associated with the intramolecular potential of an isolated molecule in the gas phase. If there is no solvent, i.e., in the gas phase, the principal origin of the barrier is completely a destabilization that accompanies nuclear rearrangement necessary for the occurrence of a reaction, and the electron delocalization helps the reaction to proceed smoothly, in which the particular orbitals, i.e., the highest occupied (HO) molecular orbital (MO) and lowest unoccupied (LU) MO of the reactant species, play the principal role.[7−9] On the other hand, in the liquid phase, especially in the polar solvent case where the charge distribution of the reactant varies in the course of reaction, the latter is so influential that both the free energy of activation and the location of the TS on the FES become quite different from those in the gas phase.[10−18] So far, there have been many theoretical studies to focus on the interaction energies between the solute and solvent molecules to investigate the origin of the free energy of activation and the TS location on the FES.[5,10−14] However, there has been no study to pay attention to the entropy contribution.

The smallest amino acid, glycine, is of considerable interest for its structure, reactivity, and other properties due to its pivotal biological significance.[19,20] Those structures in the gas phase and aqueous solution are completely different from each other. According to the *ab initio* MO electronic structure investigations,[21−23] glycine is a nonionic molecule in the gas phase, and then its zwitterion (ZW) does not exist stably. Recently, Jensen and Gordon[15] have investigated how many water molecules are needed in order to stabilize the ZW in the gas phase by *ab initio* MO method; they found that at least two water molecules are enough to stabilize the ZW and then it becomes a minimum on the potential energy, adiabatic ground state, and 298 K free energy surface.

On the other hand, by using the titration method, Wada *et al.*[16] concluded that the ZW is much more stable than the neutral form (NF) in water solution by the free energy change of 7.27

* Author to whom correspondence should be addressed.
† Permanent address: Daicel Chemical Industries, Ltd., 1239, Shinzaike, Aboshi- ku, Himeji, Hyogo 671-12 Japan.

S1089-5639(98)02534-1 CCC: $15.00
Published on Web 09/24/1998

kcal/mol. Further, by determining the ratios of the ZW to the NF in the mixture of water with the organic solvents, they concluded that the free energy change of the intramolecular protonation process in glycine is controlled mainly by electrostatic interaction, especially by the entropy change associated with the preferential solvation around the charged amino and carboxyl groups. According to Monte Carlo (MC) simulations[17] in aqueous solution, the ZW is much more stable than the NF by the interaction energy change of 86.4 kcal/mol. Therefore, the potential energy surface of glycine will vary drastically as its environment changes from the gas phase to aqueous solution. In other words, it is difficult to imagine the TS geometry of the reaction from the ZW to the NF in aqueous solution, although at least we might predict that it is different from both those of the ZW in aqueous solution and NF in the gas phase very much.

There are many studies on kinetics of the intramolecular proton transfer reaction of glycine.[24−29] By various NMR relaxation techniques,[24,25] a rate constant of 175 s^{-1} was reported. By the chemical relaxation method, Slifkin and Ali[26] obtained a free energy of activation of 14.36 kcal/mol. Furthermore, by measurements of the rate constant at several temperatures, they derived enthalpy and $T\Delta S$ contributions to the free energy of activation as −0.22 and −14.57 kcal/mol, respectively.[26] Therefore, according to their experiment, it is concluded that the origin of the free energy of activation for the reaction is mainly the entropy contribution. In other words, taking into account the fact that there is no barrier in the gas phase, it can be called the *entropy* barrier due to the solvent molecules. In the present article, we will elucidate the barrier origin in aqueous solution, from the microscopic point of view, as well as the TS location for the reaction, carrying out MD simulations.

The present paper is organized as follows. After introducing the methodology for MD simulations in Section II, we will give Results and Discussion in Section III. Finally, the main results are summarized in Section IV.

II. Experimental Section

A. Reactive Potential Function. For the intramolecular proton transfer reaction of glycine in aqueous solution, not only to know the free energy of activation but also to locate the proper TS by using the MD treatment, we have employed the reactive potential energy function obtained previously by the empirical valence bond (EVB) method:[14,30,31]

$$V_{RS} = \frac{1}{2}(V_{11} + V_1^{int} + V_{22} + V_2^{int}) - \sqrt{\left(\frac{V_{11} + V_1^{int} - V_{22} - V_2^{int}}{2}\right)^2 + V_{12}{}^2} \quad (2.1)$$

where R and S denote reactant and solvent, respectively, and, V_{11} and V_{22} are the energies for the following related resonance forms, i.e., the ZW and NF, respectively:

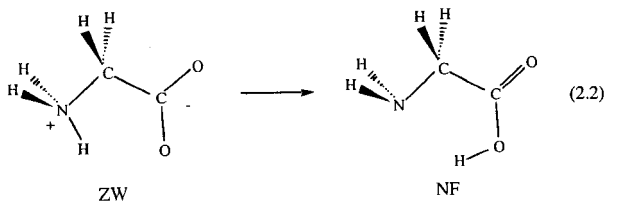

ZW NF (2.2)

According to Warshel,[30] we have adopted rather simple analytical forms for V_{11} and V_{22} by making use of the AMBER potential function.[32] Further, V_1^{int} is the interaction energy between ZW and a water molecules and V_2^{int} is that between NF and a water molecule as follows:

$$V_k^{int} = \sum_n^{solute} \sum_i^{nth\text{-}water} \sum_j \left(\frac{A_{ij}^{int(k)}}{R_{ij}^{12}} + \frac{B_{ij}^{int(k)}}{R_{ij}^{6}} + \frac{C_{ij}^{int(k)}}{R_{ij}} \right) (k = 1, 2) \quad (2.3)$$

where R_{ij} is the distance between the ith atom on the solute and the jth atom on the nth water molecule, and $A_{ij}^{int(k)}$, $B_{ij}^{int(k)}$, and $C_{ij}^{int(k)}$ are disposable parameters. From a physical point of view, we have postulated that $A_{ij}^{int(k)} > 0$. For the square of the exchange matrix element (SEME) $V_{12}{}^2$, we have adopted the analytical form that Chang and Miller (CM)[31] have recently improved, reproducing *ab initio* MO surfaces with high accuracy:

$$V_{12}{}^2 = A \exp(B^T \Delta \boldsymbol{q} - {}^1/_2 \Delta \boldsymbol{q}^T C \, \Delta \boldsymbol{q}) \quad (2.4)$$

In eq 2.4, $\Delta \boldsymbol{q} = \boldsymbol{q} - \boldsymbol{q}_0$, where $\boldsymbol{q}$ and $\boldsymbol{q}_0$ denote any geometry and the reference geometry, i.e., for instance, the TS structure, in terms of internal coordinates. Further, A, B, and C are a disposable constant, vector, and matrix, respectively. Finally, we have employed the TIP4P model[33,34] for the solvent−solvent interaction potential V_{SS}, because it has a simple analytical form and gives a reasonable structural and thermodynamic description of liquid water. Therefore, the total potential function V_{tot} of the glycine−water system is as follows:

$$V_{tot} = V_{RS} + V_{SS} \quad (2.5)$$

These functions were prepared so as to reproduce a set of energies and forces calculated at the HF/6-31+G* level of theory,[14] using the GAUSSIAN92 program.[35] The relatively small basis set has been employed because the calculations of electronic energies and forces are necessary at so many points, i.e., 5250 points (97 points for V_{11}, 97 points for V_{22}, 2236 points for $V_{12}{}^2$, 1410 points each for V_1^{int} and V_2^{int}), and the extremely small barrier height of 0.563 kcal/mol is considered to be in good agreement with such results that there is no minimum corresponding to the ZW in the gas phase[22,23] for some larger basis sets than 6-31+G* and the post-SCF MO theory.

B. MD Simulation. Integration of the equation of motion was performed with the velocity Verlet method,[36] using the RATTLE algorithm[37] in order to constrain the molecular shapes of both glycine and solvent water. The number of molecules in the simulation box with one side length of 18.6 Å was 1 glycine and 213 water molecules. The mass density was set to be 0.997 g/cm^3, i.e., the experimental value for water at 300 K. We have calculated not only the solvent−solvent long-range Coulomb interaction but also the solute−solvent one using the Ewald sum technique.[38] In order to make the force calculations manageable, we have employed the potential truncation technique[39] in the Lennard-Jones potential terms for both solvent−solvent and solute−solvent interaction energies, owing to the fast falling off of the corresponding forces. Half of the side length of the box was chosen as the cutoff distance, because the forces for the Lennard-Jones potential terms were found to be almost zero at this distance. Equilibrium MD calculations of 10∼20 ps were performed, after 15 ps cooling and equilibration runs with a time step of 0.5 fs. Although a temperature control algorithm was not used, the temperatures were prepared to be 302.4 ± 9.6 K, 311.5 ± 10.2 K, and 321.7 ± 10.8 K.

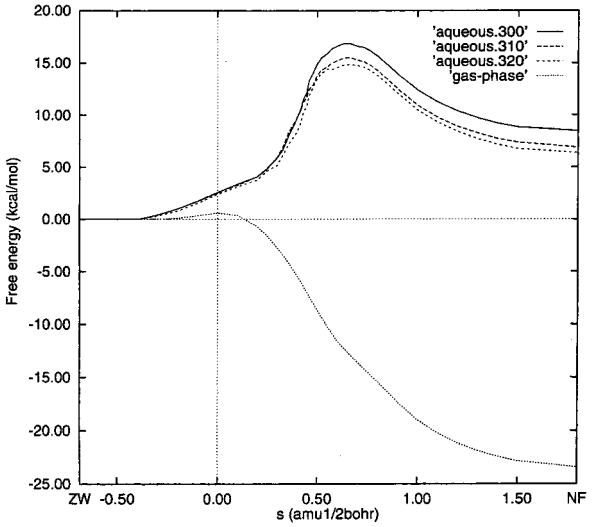

Figure 1. Free energy changes in aqueous solution at $T = 300$, 310, and 320 K (—, − − −, and ---, respectively), and the potential energy change of glycine in gas phase ΔV_R (···) along the IRC.

C. Free Energy Perturbation Theory. The free energy perturbation theory[5,30,32,40,41] provided the free energy change as the intrinsic reaction coordinate (IRC),[42] s, was varied in increments, Δs_i ($i = 1, \cdots, 27$) from $s = -0.388$ to 1.50 amu$^{1/2}$ bohr. Specifically, the free energy change for moving s_i to $s_{i+1} = s_i + \Delta s_i$ is given as follows:

$$G_{i+1} - G_i = k_B T \ln \langle \exp[-\beta\{V_{RS}(s_{i+1}) - V_{RS}(s_i)\}] \rangle_i \quad (2.6)$$

where $\beta = 1/k_B T$, $V_{RS}(s_{i+1}) - V_{RS}(s_i)$ is the energy difference between the systems at s_{i+1} and s_i, and the average is taken over the sampling at s_i. Naturally, if the reference, s_i, and perturbed, s_{i+1}, systems are too disparate, the convergence of the average in eq 2.6 becomes slow. As shown below, if we choose Δs_i larger than 0.01 amu$^{1/2}$ bohr and less than 0.10 amu$^{1/2}$ bohr, it was not problematic in the present calculations, because the standard deviations in the free energy changes of reaction and the free energies of activation are on the order of 1 kcal/mol.

III. Results and Discussion

A. TS Structure on FES. In Figure 1, ΔG(300 K), ΔG(310 K), ΔG(320 K), and ΔV_R are shown along the IRC[42] defined in the gas phase, which denote the free energy change at 300 K, 310 K, and 320 K and the corresponding reactant potential energy change in the gas phase, respectively. In the gas phase, the very small ZW−TS barrier of 0.56 kcal/mol is in good accordance with the previous results that there is no barrier by using larger basis sets.[22,23] In aqueous solution, there are maxima at $s \approx 0.66$ amu$^{1/2}$ bohr for all the temperatures, which correspond to the TS on the FES and clearly shift to the NF side, comparing with that in the gas phase. The TS geometry on the FES is, as shown in Figure 2, quite different from that of the TS in the gas phase and it is found that the TS structure in the gas phase is very close to that of the ZW in the gas phase, while that of the TS in aqueous solution is rather close to that of the NF. Qualitatively, the ZW is very unstable in the gas phase because of the charge separation into the amino and carboxyl groups, while in aqueous solution the ZW is stabilized more than the NF through the Coulomb interaction among the charged amino and carboxyl groups, and so many water molecules. However, this qualitative consideration lacks the entropy contribution. We will therefore deal with this contribution in the next subsection.

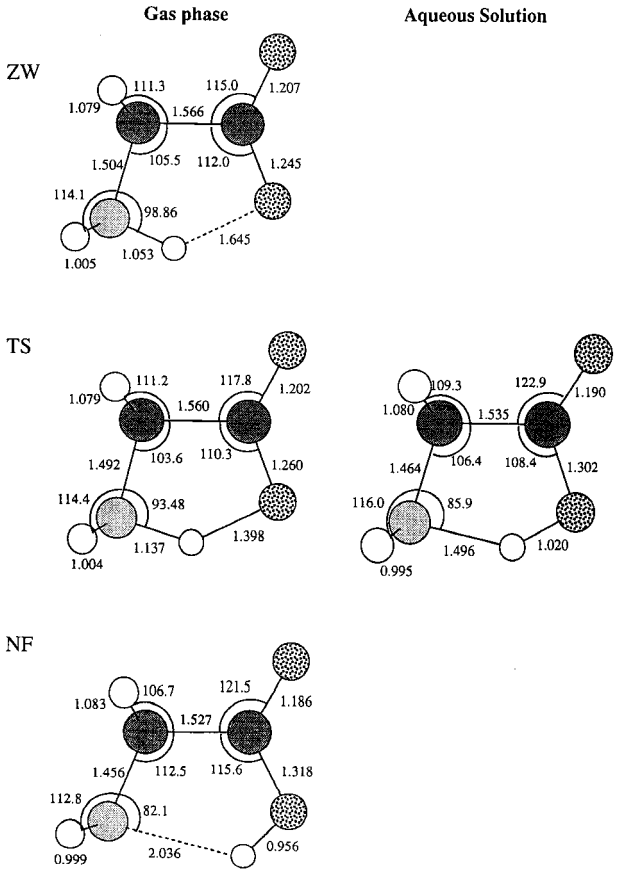

Figure 2. Bond distances and bond angles in the glycine structures in gas phase and aqueous solution. Numerical values are given in angstroms for bond lengths and in degrees for bond angles.

The difference of the free energy between the ZW and NF is 8.46 ± 1.45 kcal/mol and the free energy of activation for ZW is 16.85 ± 1.36 kcal/mol at $T = 300$ K. The corresponding experimental values are 7.27 and 14.36 kcal/mol, respectively,[16,26] which are in good agreement with ours. Further, the more the temperature increases, the more the free energy change of reaction decreases. It means that the ZW in aqueous solution is relatively destabilized in comparison to the NF as the temperature increases, which is also consistent with the results of Wada et al.[16]

B. Origin of Free Energy of Activation of FES. As shown in Figures 3 and 4, the rate and equilibrium constants are approximately correlated linearly, i.e., in so-called Arrhenius plots that plot the natural logarithm of the rate or equilibrium constant versus the reciprocal of absolute temperature.[1−4] We can obtain the enthalpy and entropy contributions, using the slopes and intercepts of the fitted lines at all points along the IRC as well as at the TS and product. In Figure 5, the enthalpy (ΔH) and entropy ($T\Delta S$) contributions are shown along the IRC at $T = 300$ K. The entropy contribution almost monotonously increases along the IRC, while the enthalpy contribution has a maximum at $s \approx 0.6$ amu$^{1/2}$ bohr. Further, the enthalpy contribution of 46.87 kcal/mol to the free energy of activation is larger than the entropy contribution of 30.12 kcal/mol. Therefore, the clear maximum of the enthalpy contribution is the origin of the free energy of activation on the FES. In Figure 6, $\langle V_{RS} \rangle$ is shown along the IRC, which denotes the average of V_{RS} corresponding to the sum of the solute potential and the interaction energy between glycine and water molecules. There is also a maximum in the energy profile of $\langle V_{RS} \rangle$ by the barrier height of ∼30 kcal/mol at $s \approx 0.6$ amu$^{1/2}$ bohr, and it

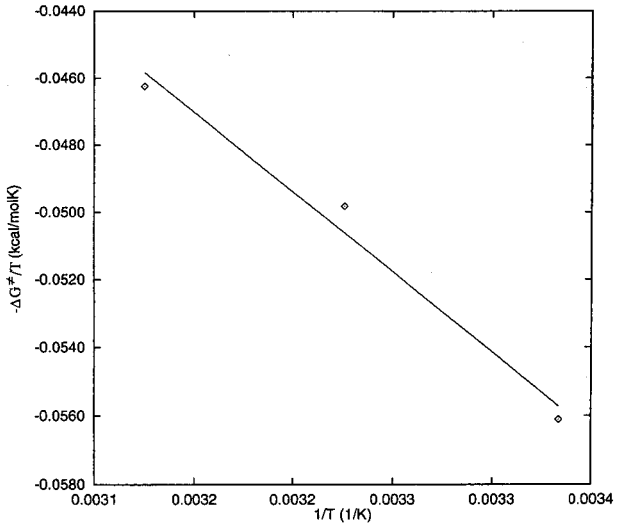

Figure 3. Plot of logarithm of the rate constant ($-\Delta G^{\ddagger}/T$) vs the inverse absolute temperature. The straight line is fitted to the plot by the least-squares method.

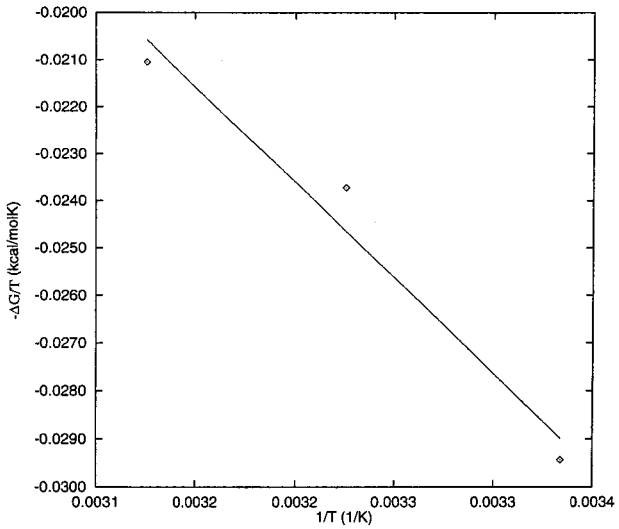

Figure 4. Plot of logarithm of the equilibrium constant ($-\Delta G/T$) vs the inverse absolute temperature. The straight line is fitted to the plot by the least-squares method.

corresponds to that of the enthalpy contribution. Thus, the reaction barrier in aqueous solution is clearly explained by the fact that, as the forward reaction (ZW → NF) proceeds, the Coulomb interaction between the charged groups of ZW and solvent water molecules becomes weaker while the intramolecular potential energy is stabilized compensatorily to form a free energy maximum.[14]

According to Slifkin and Ali,[26] the enthalpy and entropy contributions to the free energy of activation are −0.22 and −14.57 kcal/mol, respectively, which are not in agreement with our results at all. That is, experimentally, the entropy contribution mainly makes the barrier on the FES, while in our simulations the enthalpy contribution does. Qualitatively speaking, according to the compensation rule, the weaker the interaction energy between glycine and water molecules becomes as the reaction proceeds, the larger the positive entropy change does, because the configuration space accessible to the solvent water molecules becomes larger. Therefore, the positive entropy contribution is considered to become larger monotonously in the course of reaction, which supports our results. According to the results of Wada et al.,[16] the enthalpy and entropy contributions to the free energy change of reaction are

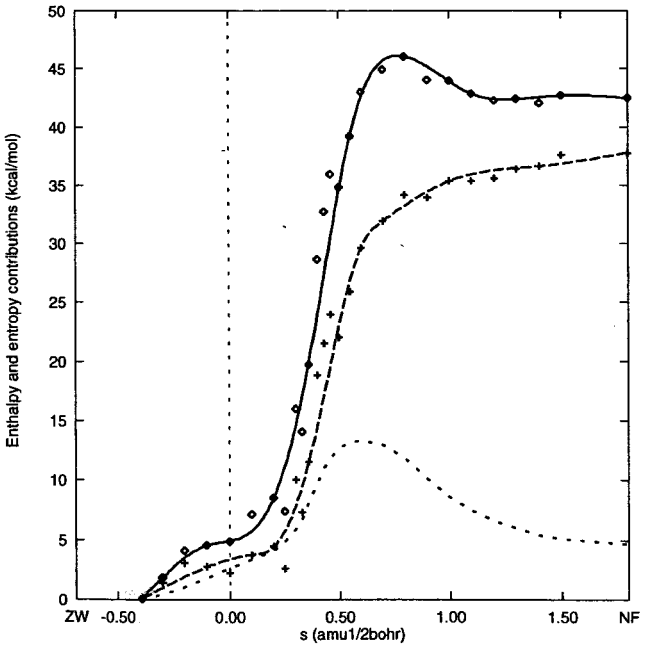

Figure 5. Enthalpy (◇) and entropy (+) contributions to the free energy changes (---) in aqueous solution at $T = 300$ K along the IRC. The curves for enthalpy (—) and entropy (− − −) ones are drawn by the natural cubic spline interpolations between the appropriate points.

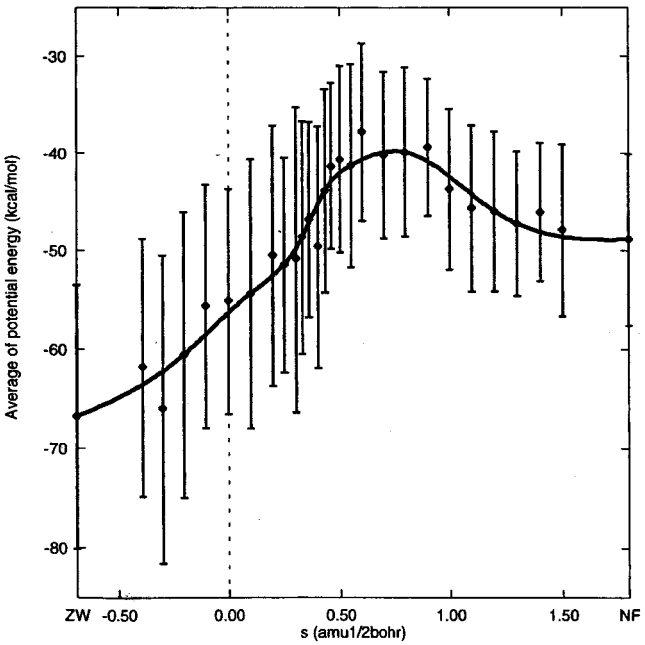

Figure 6. Averages of the potential energy $\langle V_{RS} \rangle$ along the IRC with error bars. The curve is drawn by the natural cubic spline interpolations between the appropriate points.

10.3 and 3.06 kcal/mol, respectively. The entropy change obtained by them are positive and consistent with our results (31.88 kcal/mol) and the above qualitative consideration, although our simulations have considerably overestimated it. Therefore, we conclude that the origin of the free energy of activation is the enthalpy contribution, and the compensative relationship between the monotonous decrease of the interaction energy and the decrease of the solute potential energy makes the barrier somewhere on the IRC.

C. Internal Degrees of Freedom of Reactant. So far, we have obtained the free energy profile along only a certain chosen coordinate, i.e., the IRC. That is, we have ignored the internal degrees of freedom of glycine except for the IRC. However, it

is very important to treat them for the following two reasons: (1) We should optimize in reality the TS on the FES with respect to the other internal coordinates as well as the IRC,[43] and (2) the internal degrees of freedom contribute to the free energy change because thermal energy is actually partitioned among them. With regard to the first reason, we can optimize the TS on the FES with respect to all the internal coordinates by applying the analytic gradient method[44] to the present system. Furthermore, to better describe the role of the solvent in a reaction coordinate and determine the exact free energy of activation in solution reactions, we can employ the EVB mapping approach that Warshel et al. have proposed.[30]

Regarding the second reason, as the zeroth order approximation, supposing that the two subsystems, i.e., the solute and solvent molecules, are uncorrelated,[45] we can take into account the contribution of the internal degrees of freedom of glycine as follows:[46]

$$\Delta G^{\text{total}} = \Delta G^{\text{zero}} + \Delta G^{\text{vib}} + \Delta G^{\text{inter}} \qquad (3.1)$$

where ΔG^{total} is the total change of free energy along the IRC, which consists of the zero-point vibrational energy ΔG^{zero}, the contribution of vibrational partition functions ΔG^{vib}, and that of the solvent ΔG^{inter}. ΔG^{vib} is given by[3,35]

$$\Delta G^{\text{vib}} = k_{\text{B}}T \sum_j \ln\{1 - \exp(-\beta h\nu_j)\} \qquad (3.2)$$

where h is Planck's constant, and ν_j is the jth vibrational frequency obtained at each point on the IRC by diagonalizing the projected force constant matrix that does not include the degrees of freedom of the IRC, overall translation, and rotation.[47] ΔG^{total}(300 K), ΔG^{total}(310 K), and ΔG^{total}(320 K) along the IRC have obtained, and, as a whole, each curve of the free energy change ΔG^{total} resembles that of ΔG, respectively, for all temperatures. The free energy change of reaction and the free energy of activation at $T = 300$ K are 8.81 ± 1.55 and 14.74 ± 1.26 kcal/mol, respectively. The calculated value of the free energy of activation becomes more consistent with the experimental one (14.36 kcal/mol) than that without the contribution of the internal degrees of freedom. By the temperature dependence of the free energy change, we have obtained the enthalpy and entropy contributions along the IRC, including the internal degrees of freedom. The enthalpy and entropy contributions are also very similar to those without the internal degrees of freedom. Therefore, the internal degrees of freedom have little effect on the enthalpy and entropy ones, so that the conclusion does not change that the origin of the free energy of activation on the FES is the maximum in the enthalpy one.

Despite the consideration of the internal degrees of freedom, the enthalpy and entropy contributions are 44.23 and 29.82 kcal/mol for the free energy of activation and 38.23 and 30.55 kcal/mol for the free energy change of reaction, respectively, which are still overestimated considerably. This may be due to the deficiency of the number of MD steps to calculate the free energy change. Further, in general, it is more difficult to calculate the enthalpy and entropy contributions than the corresponding free energy change, because their statistical errors are compensated by each other to evaluate the free energy, but their errors themselves are not reduced. On the other hand, as is shown in Figure 5, the calculated values obey the compensation rule at least qualitatively. Therefore, the improvement of such values has not been carried out by further statistics.

D. Microscopic Analysis of Free Energy of Activation. In the previous section, we have elucidated the TS origin on the FES for the reaction in terms of thermodynamics and energetics. In this section, we will analyze the origin differently from the microscopic point of view. That is to say, the enthalpy contribution, especially the average of the interaction energy between glycine and water molecules, will be individually analyzed. In Figure 7, the distribution functions of the interaction energy between glycine and a water molecule are shown. The ZW interacts with solvent water molecules more strongly than both the TS and NF, because the ZW consists of both positive amino and negative carboxyl groups as shown in Figure 8. Therefore, the distribution function for the ZW has relatively large values, especially in the range of strong interaction energy (about -8 to -5 kcal/mol), while those for the TS and NF are almost equal to zero. It is also understood that the distribution function for the TS is not so different from that for the NF, because the amino and carboxyl groups at the TS do not have large positive and negative charges, respectively, but have as much as that at the NF. These are the reason why the average of the interaction energy between the ZW and water molecules should be much larger than those for the TS and NF.

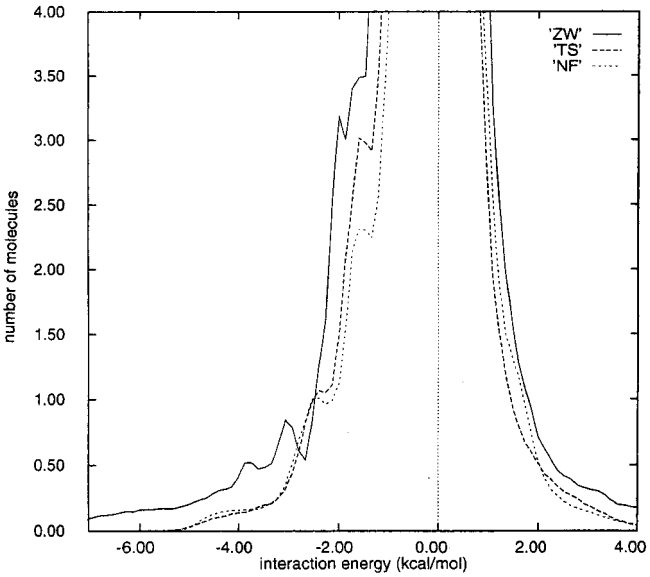

Figure 7. Distribution functions of interaction energy between glycine and a water molecule for ZW (—), TS (– – –), and NF (---) at $T =$ 300 K.

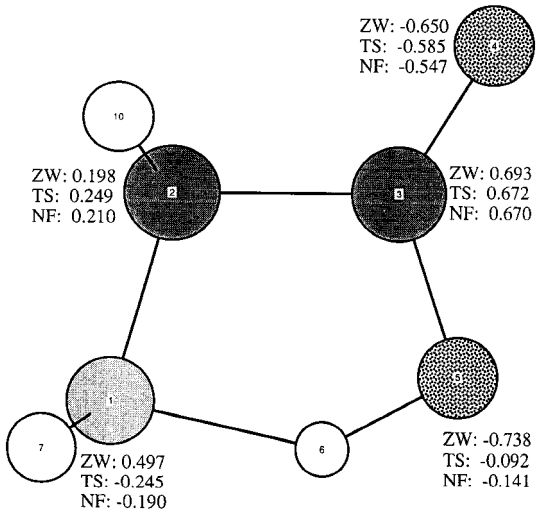

Figure 8. Partial charges of glycine for ZW, TS, and NF, which are obtained by Mulliken population analysis.

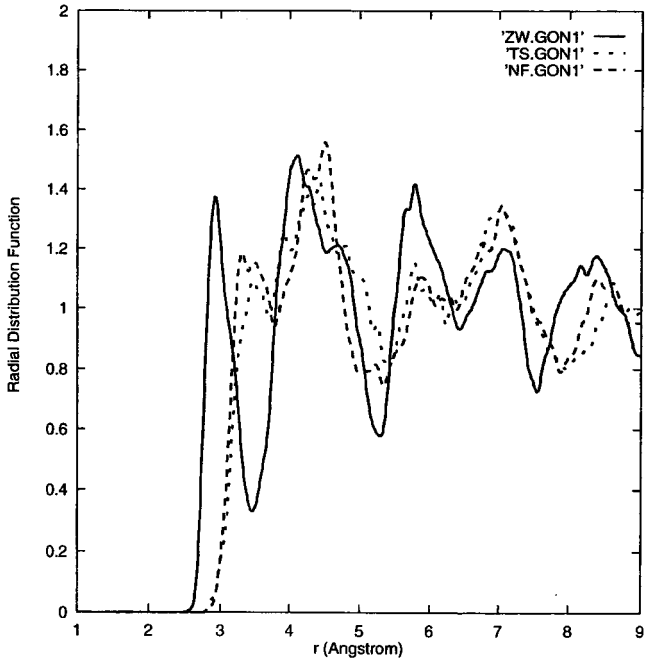

Figure 9. Radial distribution functions for the separation between the water oxygen and N1 of glycine at 300 K, for ZW (—), TS (---), and NF (– – –).

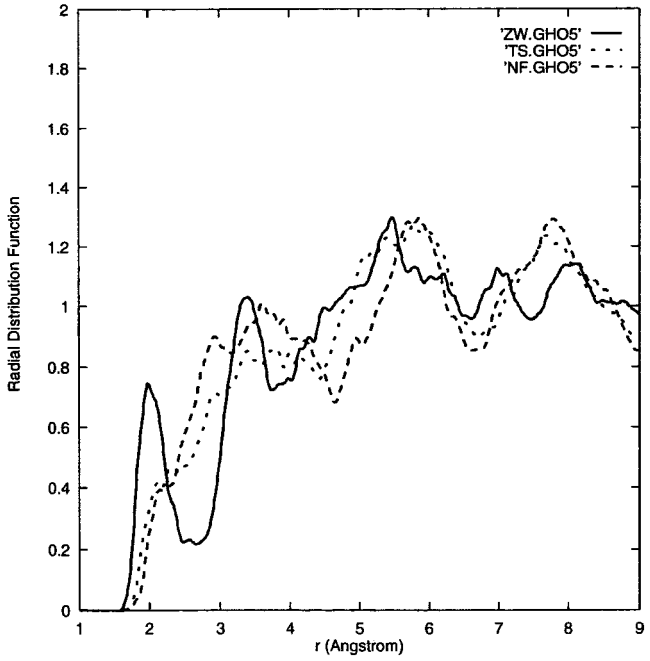

Figure 10. Radial distribution functions for the separation between the water hydrogen and O5 of glycine at 300 K, for ZW (—), TS (---), and NF (– – –).

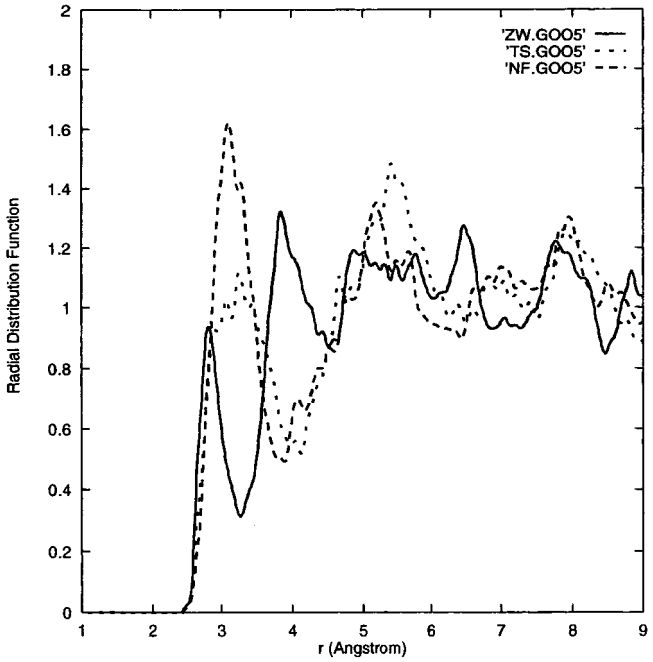

Figure 11. Radial distribution functions for the separation between the water oxygen and O5 of glycine at 300 K, for ZW (—), TS (---), and NF (– – –).

Moreover, to shed light on how the solvent molecules solvate the reactant during the reaction, i.e., how different the solvation structure around glycine at the TS is from those at the minima (the ZW and NF), in Figures 9, 10, and 11, the radial distribution functions (RDFs) g_{ON_1}, g_{HO_5}, and g_{OO_5} for ZW, TS, and NF are shown, respectively. g_{ON_1}, g_{HO_5}, and g_{OO_5} are the functions of the separations between the solvent water oxygen and N1 of glycine, the solvent water hydrogen and O5 of glycine (the oxygen of the hydroxyl group), and the solvent water oxygen and O5 of glycine, respectively. The serial numbers of the atoms in the glycine molecule are shown in Figure 8. In Figure 9, the first peaks for the ZW, TS, and NF reflect the hydrogen bondings. For the TS and NF, the first peaks are shifted to larger separation than that for the ZW, because for the TS and NF the charge of amino groups becomes smaller than that for the ZW and the interactions between the amino group and water molecules for the TS and NF are weaker than that for the ZW. As shown in Figure 10, the first peak for the ZW is very sharp. It means that the hydrogen bond is very strong because of the large negative charge of the carboxyl group. The corresponding hydrogen bonds for the TS and NF become weaker and the corresponding bond lengths become longer, because the negative charge becomes smaller than that for the ZW as the reaction proceeds. In Figure 11, the first peak for the ZW corresponds to the hydrogen bonding of the water oxygen to O5 of the solute in a linear geometry, where the oxygen−oxygen length is about 2.8 Å [= the length of the standard hydrogen bond (1.8 Å) + the length of the O−H bond of a water molecule], while the first broad peak for the NF may consist of the hydrogen bonding of the water oxygen to the O5 and O6, which is the reason why the peak is about twice as large as that for the ZW. Therefore, it is found that those water molecules that are strongly linked by hydrogen bonds to the positive amino and negative carboxyl groups for the ZW correspond to the relatively large values of the interaction energy distribution function for the ZW in the range from −8 to −5 kcal/mol. Further, as the reaction proceeds and the absolute values of the charges for the groups are smaller than those for the ZW, the water molecules that strongly linked to the groups for the ZW become rather weakly bonded to them.

IV. Summary

In this paper, for the purpose of elucidating the barrier origin in the liquid phase, i.e., the free energy of activation, and the TS location for a reaction, we have applied the MD method and free energy perturbation theory to the glycine−water system, where the potential energy surface varies drastically as its environment changes from the gas phase to aqueous solution, and experimentally there seems to be an *entropy* barrier due to the solvent molecules. It was found that the TS on the FES corresponds approximately to the geometry at $s \approx 0.66$ amu$^{1/2}$ bohr on the IRC in the gas phase, whose geometry is different from that of the TS in the gas phase very much. The free energy

difference between the ZW and NF is 8.46 ± 1.45 kcal/mol and the free energy of activation is 16.85 ± 1.36 kcal/mol at $T = 300$ K, which are in good agreement with the experimental values, respectively.

By the temperature dependence of the free energy change, we have analyzed the enthalpy and entropy contributions to the free energy change along the IRC. The entropy contribution increases almost monotonously along the IRC, while the enthalpy contribution has a maximum at $s \approx 0.6$ amu$^{1/2}$ bohr. Further, the enthalpy contribution to the free energy of activation is larger than the entropy contribution. Therefore, we conclude that the maximum of the enthalpy contribution is the origin of the free energy of activation on the FES, and the monotonous decrease of the interaction energy and the decrease of the solute potential energy in the course of reaction are compensated by each other, and the offset makes the barrier around the point.

To analyze the origin differently from the microscopic point of view, we have presented the interaction energy distribution function and the RDFs. It was found that the ZW interacts with water molecules more strongly than either the TS or the NF, especially at both the positive amino and negative carboxyl groups of the ZW. Therefore, the barrier origin in aqueous solution is attributed to the fact that the Coulomb interaction between the charged groups of the ZW and water molecules becomes weaker as the reaction proceeds, as the stabilization of the intramolecular potential energy compensates it to form a free energy maximum.

Acknowledgment. We thank Professor Kenichi Fukui for his helpful advice and discussion. The numerical calculations were carried out by using the NEC SX-4 at Institute for Fundamental Chemistry and computers at Institute for Molecular Science. This work was supported by a Grant-in-Aid for Science Research from the Ministry of Education, Science, and Culture in Japan and financially by the Research for the Future Program of the Japan Society for the Promotion of Science (Project JSPS-RFTF96P00206).

References and Notes

(1) (a) Eyring, H. *J. Chem. Phys.* **1934**, *3*, 107. (b) Wigner, E. *J. Chem. Phys.* **1937**, *5*, 720.

(2) Truhlar, D. G.; Hase, W. L.; Hynes, J. T. *J. Phys. Chem.* **1983**, *87*, 2664.

(3) Glasstone, S.; Laidler, K. J.; Eyring, H. *The Theory of Rate Processes;* McGraw-Hill: New York, 1941.

(4) Conners, K. A. *Chemical Kinetics. The Study of Reaction Rates in Solution;* VCH Publishers, Inc.: New York, 1990.

(5) (a) Jorgensen, W. L.; Ravimohan, C. *J. Chem. Phys.* **1985**, *83*, 3050. (b) Jorgensen, W. L.; Buckner, J. K. *J. Phys. Chem.* **1987**, *91*, 6083. (c) Jorgensen, W. L.; Gao, J. *J. Am. Chem. Soc.* **1988**, *110*, 4212. (d) Jorgensen, W. L. *Adv. Chem. Phys.* **1988**, *70*, 469. (e) Jorgensen, W. L. *Acc. Chem. Res.* **1989**, *22*, 184. (f) Duffy, E. M.; Severance, D. L.; Jorgensen, W. L. *J. Am. Chem. Soc.* **1992**, *114*, 7535.

(6) Hynes, J. T. In *Theory of Chemical Reaction Dynamics;* Baer, M., Ed.; CRC Press: Boca Raton, FL, 1985; Vol. IV and references therein.

(7) (a) Fukui, K. *Theory of Orientation and Stereoselection*, Springer: Berlin, 1970, 1975. (b) *The World of Quantum Chemistry. Proceedings of the First International Congress of Quantum Chemistry, Menton, 1973;* Daudel, R.; Pullman, B., Eds.; D. Reidel: Dordrecht: The Netherlands, 1974.

(8) Bader, R. F. W. *Can. J. Chem.* **1962**, *40*, 1164.

(9) Nakatsuji, H. *J. Am. Chem. Soc.* **1973**, *95*, 345.

(10) Chandrasekhar, J.; Smith, S. F.; Jorgensen, W. L. *J. Am. Chem. Soc.* **1985**, *107*, 154.

(11) Madura, J. D.; Jorgensen, W. L. *J. Am. Chem. Soc.* **1986**, *108*, 2517.

(12) Buckner, K. K.; Jorgensen, W. L. *J. Am. Chem. Soc.* **1989**, *111*, 2507.

(13) (a) Bergsma, J. P.; Gertner, B. J.; Wilson, K. R.; Hynes, J. T. *J. Chem. Phys.* **1987**, *86*, 1356. (b) Gertner, B. J.; Whitnell, R. M.; Wilson, K. R.; Hynes, J. T. *J. Am. Chem. Soc.* **1991**, *113*, 74. (c) Benjamin, I.; Gertner, B. J.; Tang, N. J.; Wilson, K. R. *J. Am. Chem. Soc.* **1990**, *112*, 524.

(14) Okuyama-Yoshida, N.; Nagaoka, M.; Yamabe, T. *J. Phys. Chem.* **1998**, *102*, 285.

(15) Jensen, J. H.; Gordon, M. S. *J. Am. Chem. Soc.* **1995**, *117*, 8159.

(16) Wada, G.; Tamura, E.; Okina, M.; Nakamura, M. *Bull. Chem. Soc. Jpn.* **1982**, *55*, 3064.

(17) (a) Romano, S.; Clementi, E. *Int. J. Quantum Chem.* **1978**, *14*, 839. (b) Clementi, E.; Cavallone, F.; Scordamaglia, R. *J. Am. Chem. Soc.* **1977**, *99*, 5531. (c) Carozzo, L.; Corongiu, G.; Petrongolo, C.; Clementi, E. *J. Chem. Phys.* **1978**, *68*, 787.

(18) Hayashi, S.; Ando, K.; Kato, S. *J. Phys. Chem.* **1995**, *99*, 955.

(19) Schuster, P.; Wolschann, P.; Tortschanoff, K. Dynamics of proton transfer in solution. In Chemical relaxation in molecular biology; Pecht, I., Rigler, R., Eds.; Springer-Verlag: Berlin, Heidelberg, 1976.

(20) Morrison, R. T.; Boyd, R. N. *Organic Chemistry*, 4th ed.; Allyn and Bacon, Inc.: Boston, MA, 1983.

(21) Tse, Y.-C.; Newton, M. D.; Vishveshwara, S.; Pople, J. A. *J. Am. Chem. Soc.* **1978**, *100*, 4329.

(22) Ding, Y.; Krogh-Jespersen, K. *Chem. Phys. Lett.* **1992**, *199*, 261.; *J. Comput. Chem.* **1996**, *17*, 338.

(23) Yu, D.; Armstrong, D. A.; Rauk, A. *Can. J. Chem.* **1992**, *70*, 1762.

(24) Sheinblatt, M.; Gutowsky, H. S. *J. Am. Chem. Soc.* **1964**, *86*, 4814.

(25) Chang, K. C.; Grunwald, E. *J. Phys. Chem.* **1976**, *80*, 1422.

(26) Slifkin, M. A.; Ali, S. M. *J. Mol. Liquids* **1984**, *28*, 215.

(27) Inoue, H. *J. Sci. Hiroshima Univ. Ser. A-II* **1970**, *34* (1), 17.

(28) Applegate, K.; Slutsky, L. J.; Parker, R. C. *J. Am. Chem. Soc.* **1968**, *90*, 6909.

(29) Hussey, M.; Edmonds, P. D. *J. Acoustical Soc. Am.* **1971**, *49*, 1309.

(30) (a) Warshel, A.; Weiss, R. M. *J. Am. Chem. Soc.* **1980**, *102*, 6218. (b) Åqvist, J.; Warshel, A. *Chem. Rev.* **1993**, *93*, 2523. (c) Warshel, A. *Computer Modeling of Chemical Reactions in Enzymes and Solutions;* John Wiley and Sons, Inc.: New York, 1991. (d) Warshel, A.: Russell, S. *J. Am. Chem. Soc.* **1986**, *108*, 6569. (e) Hwang, J.-K.; King, G.; Creighton, S.; Warshel, A. *J. Am. Chem. Soc.* **1988**, *110*, 5297.

(31) (a) Chang, Y.-T.; Miller, W. H. *J. Phys. Chem.* **1990**, *94*, 5884. (b) Miller, W. H.; Chang, Y.-T.; Makri, N. *Molecular Structure and Reactivity in Computational Advances in Organic Chemistry;* Ögretir, C., Csizmadia, I. G., Eds.; Kluwer Academic Publishers: Dordrecht, The Netherlands, 1991.

(32) (a) Singh, U. C.; Brown, F. K.; Bash, P. A.; Kollman, P. A. *J. Am. Chem. Soc.* **1987**, *109*, 1607. (b) Kollman, P. *Chem. Rev.* **1993**, *93*, 2395. (c) Kollman, P. A.; Merz, K. M., Jr. *Acc. Chem. Res.* **1990**, *23*, 246.

(33) (a) Jorgensen, W. L.; Chandrasekher, J.; Madura, J. D.; Impey, R. W.; Klein, M. L. *J. Chem. Phys.* **1983**, *79*, 926. (b) Jorgensen, W. L.; Madura, J. D. *Mol. Phys.* **1985**, *56*, 1381.

(34) Neumann, M. *J. Chem. Phys.* **1986**, *85*, 1567.

(35) Frisch, M. J.; Trucks, G. W.; Head-Gordon, M.; Gill, P. M. W.; Wong, M. W.; Foresman, J. B.; Johnson, B. G.; Schlegel, H. B.; Robb, M. A.; Replogle, E. S.; Gomperts, R.; Andres, J. L.; Raghavachari, K.; Binkley, J. S.; Gonzalez, C.; Martin, R. L.; Fox, D. J.; Defrees, D. J.; Baker, J.; Stewart, J. J. P.; Pople, J. A. *Gaussian 92*, Revision C.4; Gaussian Inc.: Pittsburgh, PA, 1992.

(36) (a) Verlet, L. *Phys. Rev.* **1967**, *159*, 98. (b) Swope, W. C.; Andersen, H. C.; Berens, P. H.; Wilson, K. R. *J. Chem. Phys.* **1982**, *76*, 637. (c) Humphreys, D. D.; Friesner, R. A.; Berne, B. J. *J. Phys. Chem.* **1994**, *98*, 6885.

(37) Andersen, H. C. *J. Comput. Phys.* **1983**, *52*, 24.

(38) Ewald, P. *Ann. Phys.* **1921**, *64*, 253.

(39) Allen, M. P.; Tildesley, D. J. *Computer Simulation of Liquids*, Oxford University Press: Oxford, England, 1987.

(40) Zwanzig, R. W. *J. Chem. Phys.* **1954**, *22*, 1420.

(41) Torrie, G. M.; Valleau, J. P. *Chem. Phys. Lett.* **1974**, *28*, 578.

(42) (a) Fukui, K. *J. Phys. Chem.* **1970**, *74*, 461; (b) *Acc. Chem. Res.* **1981**, *14*, 363.

(43) Okuyama-Yoshida, N.; Nagaoka, M.; Yamabe, T. Manuscript in preparation.

(44) (a) Schlegel, H. B. *Adv. Chem. Phys.* **1987**, *67*, 249; (b) *J. Comput. Chem.* **1982**, *3*, 214.

(45) Smith, P. E.; van Gunsteren, W. F. *J. Phys. Chem.* **1994**, *98*, 13735.

(46) In eq 3.1, assuming that the internal degrees of freedom are quantized because of their high vibrational frequencies, we have dealt with only the zero-point vibrational energy and the contributions of vibrational partition functions. The further quantum mechanical treatment for the tunneling and mode quantization effects has been disccussed by Voth et al., employing the path integral approach. (a) Voth, G. A.; Chandler, D.; Miller, W. H. *J. Phys. Chem.* **1989**, *93*, 7009. (b) Li, D.; Voth, G. A. *J. Phys. Chem.* **1991**, *95*, 10425. (c) Voth, G. A. *J. Phys. Chem.* **1993**, *97*, 8365.

(47) Miller, W. H.; Handy, N. C.; Adams, J. E. *J. Chem. Phys.* **1980**, *72*, 99.